Mechanism of the modulation of BK potassium channel complexes with different auxiliary subunit compositions by the omega-3 fatty acid DHA

Toshinori Hoshi[a,1], Yutao Tian[a], Rong Xu[a], Stefan H. Heinemann[b], and Shangwei Hou[c]

[a]Department of Physiology, University of Pennsylvania, Philadelphia, PA 19104; [b]Center for Molecular Biomedicine, Department of Biophysics, Friedrich Schiller University and Jena University Hospital, D-07745 Jena, Germany; and [c]Key Laboratory of Systems Biomedicine, Shanghai Center for Systems Biomedicine, Shanghai Jiao Tong University, Shanghai, China 200240

Edited by Ramon Latorre, Centro Interdisciplinario de Neurociencias, Universidad de Valparaíso, Valparaíso, Chile, and approved January 29, 2013 (received for review December 17, 2012)

Large-conductance Ca^{2+}- and voltage-activated K^+ (BK) channels are well known for their functional versatility, which is bestowed in part by their rich modulatory repertoire. We recently showed that long-chain omega-3 polyunsaturated fatty acids such as docosahexaenoic acid (DHA) found in oily fish lower blood pressure by activating vascular BK channels made of Slo1+β1 subunits. Here we examined the action of DHA on BK channels with different auxiliary subunit compositions. Neuronal Slo1+β4 channels were just as well activated by DHA as vascular Slo1+β1 channels. In contrast, the stimulatory effect of DHA was much smaller in Slo1+β2, Slo1+LRRC26 (γ1), and Slo1 channels without auxiliary subunits. Mutagenesis of β1, β2, and β4 showed that the large effect of DHA in Slo1+β1 and Slo1+β4 is conferred by the presence of two residues, one in the N terminus and the other in the first transmembrane segment of the β1 and β4 subunits. Transfer of this amino acid pair from β1 or β4 to β2 introduces a large response to DHA in Slo1+β2. The presence of a pair of oppositely charged residues at the aforementioned positions in β subunits is associated with a large response to DHA. The Slo1 auxiliary subunits are expressed in a highly tissue-dependent fashion. Thus, the subunit composition-dependent stimulation by DHA demonstrates that BK channels are effectors of omega-3 fatty acids with marked tissue specificity.

$K_{Ca}1.1$ | fish oil | lipids

Large-conductance Ca^{2+}- and voltage-gated K^+ (Slo1 BK) channels play physiologically critical roles in numerous cell types such as neurons, endocrine cells, and muscle cells (1). This functional versatility of Slo1 BK channels is conferred by diverse mechanisms including tissue-specific coassembly of the pore-forming subunit Slo1 with its auxiliary subunits (2). To date, two major classes of Slo1 auxiliary subunits have been identified: β and γ [leucine-rich repeat containing (LRRC) proteins] subunits (2–4). Slo1 BK channel complexes containing β4 subunits (Slo1+β4) are found abundantly in neurons where they regulate action potentials and neurotransmitter release (5, 6). Slo1+β1 channels are present in smooth muscle cells (7) and activation of the channels promotes muscle relaxation (8). Accordingly, genetic disruptions of Slo1+β1 channels in mice can lead to multiple pathologies including hypertension (9) and overactive bladder (10, 11). Furthermore, a nonsynonymous polymorphism in the human β1 gene alters airway smooth muscle tone and asthma susceptibility (12).

Structurally, β subunits contain two transmembrane segments (TM1 and TM2) connected with an extracellular linker, placing the N and C termini on the intracellular side (13). Up to four β subunits may be associated with a tetrameric Slo1 channel (7, 14). Each β subunit likely positions itself between two neighboring voltage-sensor domains of the Slo1 channel so that the extracellular side of TM1 is adjacent to S1 and S2 of one pore-forming Slo1 subunit and that the extracellular end of TM2 is close to S0 of another Slo1 subunit (15–17).

Inclusion of the auxiliary subunits in Slo1 BK channel complexes markedly alters their cellular targeting, pharmacological properties, and gating characteristics (2, 3, 6, 9, 18, 19). For example, activation and deactivation kinetics of Slo1+β1 and Slo1+β4 channels are markedly slower than those of Slo1 alone without any auxiliary subunit (hereafter referred to as Slo1 channels) (5) and the apparent Ca^{2+} sensitivity of Slo1+β1 channels is also greater (20, 21). Additionally, modulatory characteristics of Slo1+β1 channels often differ from those of Slo1 channels (22–24). The BK channel activator dehydrosoyasaponin-I originally isolated from a medicinal herb (25) preferentially activates Slo1+β1 channels (22), and stress steroids acutely activate Slo1+β4 more readily than Slo1+β2 or Slo1 (26). Further, exogenous phosphatidylinositol 4, 5-bisphosphate (PIP_2) is noticeably more effective in stimulating Slo1+β1 than Slo1+β4 (24).

We previously demonstrated that vascular Slo1+β1 channels are robustly and reversibly activated by DHA (27), a long-chain polyunsaturated omega-3 fatty acid with a 22-carbon chain (for structure, see Fig. 1*A*) found abundantly in oily fish (28). Injection of DHA into wild-type mice but not in Slo1 knockout mice significantly lowers blood pressure, clearly confirming the physiological significance of DHA-mediated modulation of Slo1+β1 channels (27). In addition to the roles in the cardiovascular system (29), omega-3 fatty acids are also important in other systems. For instance, DHA is essential for normal development and function of the brain (30). Deficiency of DHA in the nervous system impairs synaptic transmission (31) and DHA supplementation may be protective against neurodegenerative diseases and psychiatric disorders (32, 33).

Expression of Slo1 β and γ subunits is tissue dependent (2) and if any auxiliary subunit-dependent effect of DHA on Slo1 BK channel complexes exists, such a finding will have important implications in the physiological action of DHA. We therefore compared the effects of DHA on Slo1 BK channels with different auxiliary subunit compositions. A large stimulatory effect of DHA was observed in Slo1+β1 and Slo1+β4 but not in Slo1+β2, Slo1+LRRC26 (γ1), or Slo1 alone. The differential effects among Slo1+β1, Slo1+β4, and Slo1+β2 to DHA are traced to two amino acid residues: one in the N terminus and the other in the N-terminal end of TM1. Oppositely charged amino acids at these locations confer large responses to DHA in the resulting Slo1+β complexes.

Author contributions: T.H., Y.T., S.H.H., and S.H. designed research; T.H., Y.T., R.X., and S.H. performed research; T.H., Y.T., S.H.H., and S.H. analyzed data; and T.H., Y.T., S.H.H., and S.H. wrote the paper.

The authors declare no conflict of interest.

This article is a PNAS Direct Submission.

[1]To whom correspondence should be addressed. E-mail: hoshi@hoshi.org.

This article contains supporting information online at www.pnas.org/lookup/suppl/doi:10.1073/pnas.1222003110/-/DCSupplemental.

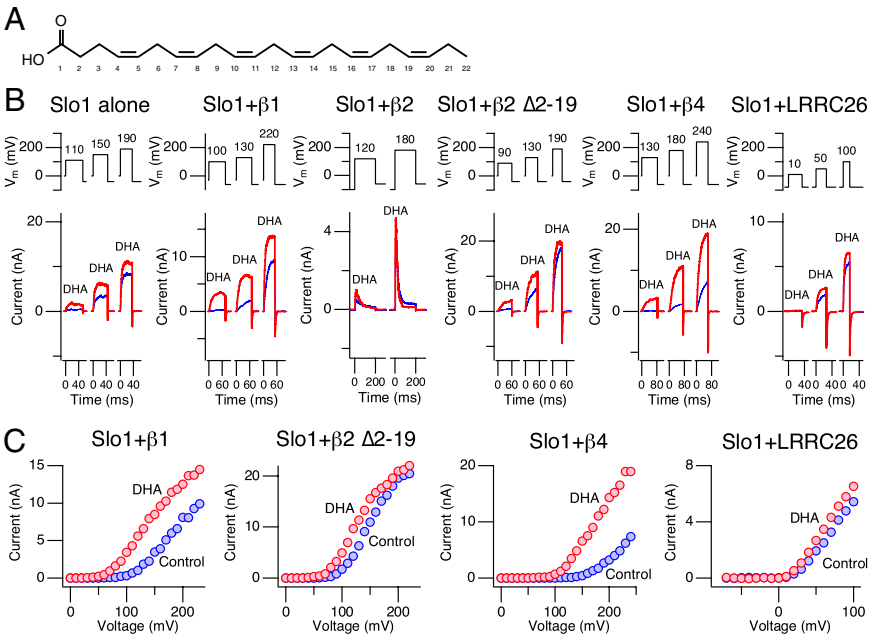

Fig. 1 Differential effects of DHA on Slo1 BK channels with various auxiliary subunits. (*A*) Structure of DHA (docosahexaenoic acid). (*B*) Representative currents elicited by pulses to different voltages in inside-out patches without Ca^{2+} through channels composed of Slo1 alone, Slo1+β1, Slo1+β2, Slo1+β2 Δ2–19, Slo1+β4, and Slo1+LRRC26 (γ1). In each panel, currents before (blue) and after (red) application of DHA (3 μM) are shown. Pulses were applied every 2 s except for Slo1+β2, which was stimulated every 10 s. For Slo1+β2, 1-s prepulses to −100 mV preceded depolarization pulses. For Slo1+LRRC26 (γ1), the holding voltage was −80 mV. (*C*) Representative peak IV curves from Slo1+β1, Slo1+β2 Δ2–19, Slo1+β4, and Slo1+LRRC26 (γ1). Results before (blue) and after (red) application of DHA (3 μM) are shown. All results were obtained in the virtual absence of Ca^{2+}.

Results

Functional diversity of BK channels is in part conferred by cell-specific assembly of pore-forming Slo1 subunits with various auxiliary β and γ subunits (2, 34). We showed previously that DHA increased currents through native BK channels in vascular smooth muscle cells as well as heterologously expressed Slo1+β1 channels (27). Here we examined whether DHA stimulates Slo1 channels with other subunit compositions: Slo1 alone, Slo1+β2 (18, 19), Slo1+β4 (6), and Slo1+LRRC26 (γ1) (3, 4). Because coassembly with wild-type β2 introduces inactivation mediated by the β2 N terminus in the resulting channel complex (35), we also examined the impact of β2 with a deletion in the N terminus (Δ2–19) to remove inactivation (18, 19). Pore-forming Slo1 and auxiliary subunits were coexpressed in human embryonic kidney (HEK) cells and studied using the inside-out patch-clamp method. Functional coassembly of Slo1 and the auxiliary subunits was confirmed in each patch by examining the characteristic gating changes conferred (Fig. S1). Representative ionic currents recorded before and after application of DHA (3 μM), a functionally saturating concentration in Slo1+β1 (27), are shown in Fig. 1*B*. The increase in peak outward current size was most readily observed in Slo1+β1 and Slo1+β4 channels, and it was much less noticeable in Slo1+β2, Slo1+β2 Δ2–19, and Slo1+LRRC26 (γ1) (Fig. 1*C*). The differential effects of DHA in Slo1+β1, Slo1+β2 Δ2–19, and Slo1+β4 are particularly noteworthy because β1, β2, and β4 share a relatively similar amino acid sequence and structural organization.

In Slo1+β1 and Slo1+β4 channels, DHA increased peak currents by up to 20- to 30-fold at select voltages, whereas the increase was limited to only a few-fold in Slo1+β2 Δ2–19 (Fig. 2, first row). The differential effects of DHA among the three channel types were also evident in comparison with the normalized conductance-voltage (*GV*) curves before and after application of DHA (Fig. 2, second row). DHA caused nearly a 60-mV shift in *GV* to the negative direction in Slo1+β1 and Slo1+β4 but the shift was much more limited in Slo1+β2 Δ2–19. Furthermore, DHA altered the activation and deactivation kinetics of the three channel types differentially. In Slo1+β1 and Slo1+β4, DHA caused a readily noticeable acceleration of the activation kinetics in the voltage range of 100–200 mV (Fig. 2, third row), decreasing the time constant by up to ∼3.5-fold (Fig. 2, fourth row). The effect of DHA on the activation kinetics in Slo1+β2 Δ2–19 was only modest; the time constant decreased by only ∼30%. In contrast with the obviously dissimilar effects of DHA on the activation kinetics of the three channel types, DHA moderately slowed the deactivation kinetics in all three channels at negative voltages by ∼50% (Fig. 2, third and fourth rows).

Changes in voltage-dependent activation properties caused by DHA in the different channel types are summarized in Fig. 3*A*.

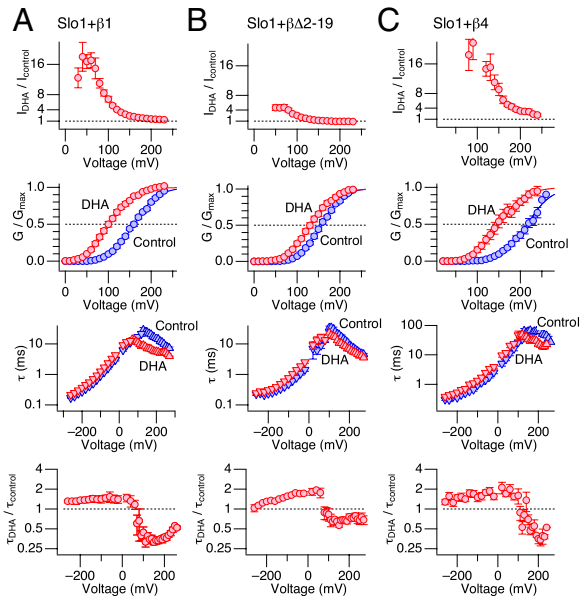

Fig. 2. Changes in gating properties of Slo1+β1 (*A*), Slo1+β2 Δ2–19 (*B*), and Slo1+β4 (*C*) caused by DHA (3 μM) without Ca^{2+}. For each channel type (from *Top* to *Bottom*), the fractional increase in peak outward current by DHA, normalized *GV* curves before (blue) and after (red) application of DHA, time constants of current relaxation before (blue) and after (red) application of DHA, and the fractional increase in time constant by DHA are shown. $n = 4–11$. In the *GV* panels, the smooth curves are Boltzmann fits to the results with $V_{0.5} = 160.0 \pm 1.0$ mV and $Q_{app} = 0.90 \pm 0.04$ (control) and 102.7 ± 1.7 mV and 0.93 ± 0.05 (DHA) in *A*, $V_{0.5} = 156.9 \pm 1.0$ mV and $Q_{app} = 1.05 \pm 0.04$ (control), and 131.6 ± 1.2 mV and 0.96 ± 0.04 (DHA) in *B*, and $V_{0.5} = 216.3 \pm 2.2$ mV and $Q_{app} = 0.88 \pm 0.07$ (control) and 150.2 ± 2.3 mV and 0.82 ± 0.06 (DHA) in *C*. All results were obtained in the virtual absence of Ca^{2+}.

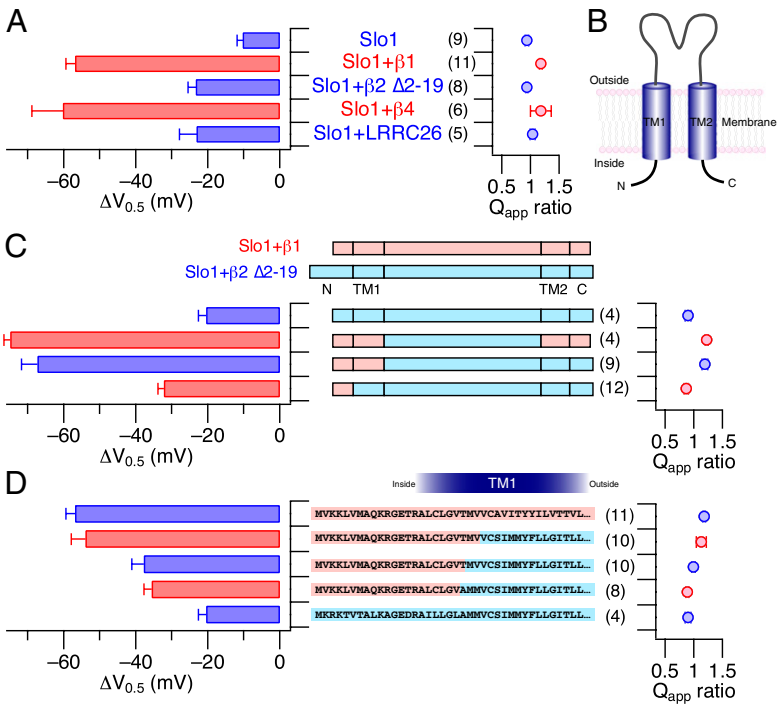

Fig. 3. Changes in steady-steady activation properties by DHA in different Slo1 channel complexes. (*A*) $\Delta V_{0.5}$ and fractional changes in Q_{app} in the channels indicated. The $\Delta V_{0.5}$ values for Slo1+β1 and Slo1+β4 differ from those for Slo1+β2 Δ2–19 and Slo1+LRRC26 (γ1), which are in turn different from those for Slo1 alone ($P < 0.05$). The Q_{app} ratio values were statistically indistinguishable among the channel types. (*B*) Structural organization of β subunits. (*C*) $\Delta V_{0.5}$ and fractional changes in Q_{app} in Slo1+β1–β2 chimeric constructs. The $\Delta V_{0.5}$ results for the *Middle* two chimeras are different from the *Top* and the *Bottom* chimera, which are in turn different from each other ($P < 0.05$). (*D*) $\Delta V_{0.5}$ and fractional changes in Q_{app} in the chimeric constructs targeting the N terminus and TM1. Based on the $\Delta V_{0.5}$ values, the *Upper* two channels, the third and fourth channels, and the *Lower* channel constitute three statistically distinct groups ($P < 0.05$). In *C* and *D*, pink regions in the structural cartoons represent β1 segments, and light blue areas represent β2 segments. All results are from inside-out experiments with 3 μM DHA in the virtual absence of Ca^{2+}.

Clearly, the shift in *GV* $V_{0.5}$ ($\Delta V_{0.5}$) by DHA was markedly greater in Slo1+β1 and Slo1+β4. Fractional changes in the steepness of GV (Q_{app} ratio) did not vary significantly among the different channels. To reveal the molecular elements within the β1 subunit critical for the prominent stimulatory effect of DHA in Slo1+β1 in contrast with the smaller effect in Slo1+β2 Δ2–19, we used chimeric β subunits based on β1 and β2 Δ2–19. Each β subunit possesses two transmembrane segments (TM1 and TM2) connected by an extracellular linker such that the N and C termini face the intracellular side (Fig. 3*B*) (36). When both the N terminus and the TM1 segment of β1 were present in the β2 background, a large $\Delta V_{0.5}$ was observed (Fig. 3*C*). The fractional increase in peak current size and changes in the channel kinetics by DHA in this mutant were also virtually identical to those in Slo1+β1 channels (Fig. S2). However, the β1 N terminus alone was not sufficient to confer the full response to DHA because inclusion of only the β1 N terminus in the β2 background without β1 TM1 produced a $\Delta V_{0.5}$ of −32.2 ± 1.6 mV, which is significantly smaller than the $\Delta V_{0.5}$ for Slo1+β1 (Fig. 3*C*). In addition, the fractional increase in current plateaued around eightfold and the acceleration of the activation kinetics was also less pronounced than that in Slo1+β1 (Fig. S2*A*).

Measurements with additional β1–β2 chimeras involving the N terminus and the TM1 segment revealed that the N terminus and the cytoplasmic N-terminal half of TM1 in β1 confer the full response to DHA (Fig. 3*D* and Fig. S2*B*). In particular, the presence of the first 24 residues from β1, up to Val24, in the β2 background allows the resulting channel complex to respond to DHA in a manner indistinguishable from that by Slo1+β1 (Fig. 3*D*, second row and Fig. S2*B*, *Left*).

To identify the individual residues within the β1 N terminus and TM1 critical for the DHA effect, point mutations were introduced, substituting an amino acid in β1 with that in β2 at the corresponding location (Fig. 4*A*). Among these β1-to-β2 mutations in β1, V2K, L5T, M7T, Q9L, and T14D did not significantly alter the large $\Delta V_{0.5}$ value (Fig. 4*B*) or the changes in kinetics induced by DHA.

The β1-to-β2 mutation β1 R11A in the N terminus preserved the slow kinetics and the enhanced Ca^{2+}-dependent activation characteristic of Slo1 channel complexes made of Slo1 and β1 subunits (Fig. S3 *A* and *B*). However, the mutation dramatically diminished $\Delta V_{0.5}$ by DHA to the level indistinguishable from that observed with β2 Δ2–32 (Fig. 4*B* and Fig. S3 *A* and *B*). The β1 R11A mutation also rendered the activation kinetics essentially insensitive to DHA (Fig. S3*A*). Similar markedly diminished responses to DHA were observed with the charge-neutralization β1 mutants R11A, R11V, and R11G as well as the charge-reversal β1 mutants R11D and R11E (Fig. 4*C* and Fig. S3*B*). In the charge-conservative β1 mutant R11K, $\Delta V_{0.5}$ and other electrophysiological changes by DHA were large and indistinguishable from those found with the wild-type β1 subunit (Fig. 4C and Fig. S3*B*). The robust responses to DHA observed with Arg or Lys at β1 position 11 (wild-type β1 and β1 R11K) highlight the importance of a positively charged side chain at this location in tuning the response to DHA.

The β1-to-β2 mutation β1 C18L as well as β1 C18D and C18K in TM1 failed to produce functional Slo1+β1 complexes. The cells transfected with the plasmids encoding for Slo1 and these mutant β1 subunits exhibited no functional BK channel currents or currents that looked indistinguishable from the currents recorded from the cells transfected with Slo1 alone. The mutants β1 C18E, C18M, and C18R, all of which harbor a polar or charged side chain at position 18, were functional and produced large DHA-induced $\Delta V_{0.5}$ values (Fig. 4*D* and Fig. S3*C*), hinting that the presence of a polar side chain at position 18 in β1 may be critical.

The importance of β1 positions 11 and 18 together in conferring the robust response to DHA, as observed with wild-type β1, is evidenced in the β2-to-β1 double mutant β2 Δ2–32 A42R:L49C containing the same number of amino acid residues in its N terminus as in β1. In this mutant, A42 in the β2 Δ2–32 background, equivalent to position 11 in β1, and L49, equivalent to position 18 in β1, are respectively mutated to Arg and Cys as found in wild-type β1 (Fig. 4*A*). With these β2-to-β1 mutations, DHA now produced a large $\Delta V_{0.5}$ and marked changes in the activation kinetics in Slo1+β2 Δ2–32 that are essentially indistinguishable from those observed in Slo1+β1 (Fig. 4*E*, *Upper* and *H*). The peak outward current increased by about 20-fold, the *GV* curve shifted by −63.4 ± 4.3 mV (8), and the activation time constant accelerated by up to 4-fold (Fig. 4*H*). Thus, the presence of

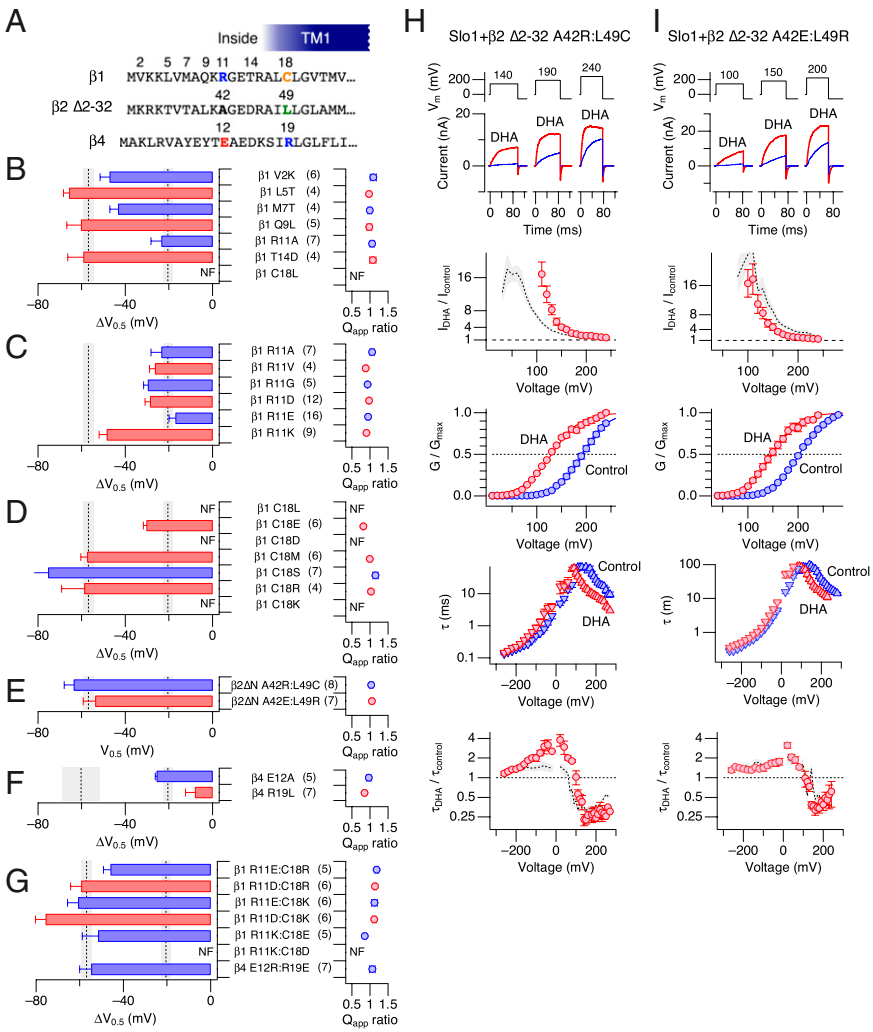

Fig. 4. Positions 11 and 18 in β1 are important for DHA sensitivity. (*A*) N-terminal and TM1 sequences of β1, β2 Δ2–32, and β4. In *B*–*G*, $\Delta V_{0.5}$ and ratios of Q_{app} in β1-to-β2 mutants (*B*), β1 R11 mutants (*C*), β1 C18 mutants (*D*), β2-to-β1/β4 mutants (*E*), β4-to-β2 mutants (*F*), and charge-pair double mutants (*G*) are shown. The gray shaded areas represent the mean ± SEM in Slo1+β1 and Slo1+β2 Δ2–19 (*B*–*E*, and *G*) and Slo1+β4 and Slo1+β2 Δ2–19 (*F*) for comparison. NF, nonfunctional—currents from cells transfected with these constructs were indistinguishable from those transfected with Slo1 alone. In *B*, only the $\Delta V_{0.5}$ values for Slo1+β1 R11A are different from all others and Slo1+β1 ($P < 0.05$) but indistinguishable from those for Slo1+β2 Δ2–32 ($P < 0.05$). In *C*, only the $\Delta V_{0.5}$ values for R11K are different from those for other mutants, which in turn are indistinguishable from those for Slo1+β2 Δ2–32 ($P < 0.05$). In *D*, the $\Delta V_{0.5}$ values for C18E are greater than those for Slo1+β2 Δ2–32 but smaller than those for Slo1+β1 ($P < 0.05$). In *E*, β2Δ*n* = β2 Δ2–32. (*H*) Changes in gating of Slo1+β2 Δ2–32 A42R:L49C possessing β2-to-β1 mutations in the β2 background by DHA (3 μM). From *Upper* to *Lower*, representative currents before (blue) and after (red) application of DHA, fractional increases in peak current size, *GV* curves, time constants of current relaxation, and fractional increases in time constant of current relaxation are shown. The gray areas, when present, represent the results (mean ± SEM) obtained from Slo1+β1. n = 4–8. In the *GV* panel, the smooth curves are Boltzmann fits to the results with $V_{0.5}$ = 192.1 ± 0.8 mV and Q_{app} = 0.98 ± 0.03 (control) and 129.9 ± 2.4 mV and 0.87 ± 0.07 (DHA). (*I*) Changes in gating of Slo1+β2 Δ2–32 A42R:L49C possessing β2-to-β4 mutations in the β2 background by DHA (3 μM). Graphs shown are as in *H*. Gray areas, when present, represent the results (mean ± SEM) obtained from Slo1+β4. n = 5–7. In the *GV* panel, the smooth curves are Boltzmann fits to the results with $V_{0.5}$ = 202.2 ± 1.0 mV and Q_{app} = 0.99 ± 0.03 (control) and 148.9 ± 1.7 mV and 0.94 ± 0.06 (DHA). All results are from inside-out experiments with 3 μM DHA without Ca^{2+}.

Arg and Cys at the β1 equivalent positions 11 and 18, as in β2 Δ2–32 A42R:L49C, is sufficient to confer the full response to DHA.

Glu12 and Arg19 in β4 correspond to Arg11 and Cys18 in β1, and to Ala42 and Leu49 in β2, respectively (Fig. 4*A*). As expected from the observation that DHA produces a large $\Delta V_{0.5}$ in Slo1+β4 but not in Slo1+β2 Δ2–32, the β4-to-β2 single mutations β4 E12A and β4 R19L markedly decreased the DHA-induced $\Delta V_{0.5}$ in Slo1+β4; the $\Delta V_{0.5}$ values in Slo1+β4 E12A and Slo1+β4 R19L were statistically indistinguishable from those in Slo1+β2 Δ2–32 (Fig. 4*F* and Fig. S3*D*). Conversely and importantly, when the β2-to-β4 double mutation A42E:L49R was introduced into the β2 Δ2–32 background, DHA introduced a large $\Delta V_{0.5}$ similar to that in Slo1+β4 (Fig. 4*E* *Lower* and *I*). The fractional increase in current and acceleration of the activation kinetics in Slo1+β2 Δ2–32 A42E:L49R also closely resembled those in Slo1+β4 (Fig. 4*I*). The amino acid positions equivalent to β1 11 and 18 must be crucial across multiple β subunit types.

Because DHA produces a large $\Delta V_{0.5}$ in both Slo1+β1 and Slo1+β4, β1-to-β4 mutations at positions 11 and 18 in β1 should preserve the large DHA-induced $\Delta V_{0.5}$ in Slo1+β1. A large $\Delta V_{0.5}$ by DHA was indeed observed in Slo1 channels with the β1-to-β4 mutant β1 C18R (Fig. 4*D*, sixth row). However, with the β1-to-β4 mutant β1 R11E, only a small $\Delta V_{0.5}$ was found (Fig. 4*C*, fifth row). When the two β1-to-β4 mutations β1 R11E and C18R were present together, a large β1-like $\Delta V_{0.5}$ was restored (Fig. 4*G*, *Top* row). The observation that the contemporaneous presence of negatively charged Glu at position 11 and positively charged Arg at position 18 of β1 as in the double mutant β1 R11E:C18R is associated with a large $\Delta V_{0.5}$ prompted us to examine the impact of other pairs of oppositely charged amino acids at these positions. Large $\Delta V_{0.5}$ values were also observed in the β1 double mutants R11D:C18R, R11E:C18K, R11D:C18K, and R11K:C18E (Fig. 4*G*), all of which pair a negatively charged amino acid and a positively charged amino acid at positions 11 and 18 in β1. The importance of such residues at positions 11 and 18 in β1 is further suggested by the finding that a large $\Delta V_{0.5}$ was maintained with β4 E12R:R19E, which exchanges the positively and negatively charged residues at the two positions in β4 (Fig. 4*G*, *Bottom* row).

Discussion

The health-promoting potential of long-chain omega-3 fatty acids has been widely touted. Reports documenting the effects of omega-3 fatty acids in a variety of organ and tissue systems abound. However, the identities of the molecular effectors of omega-3 fatty acids and the mechanisms of the interactions are only beginning to be elucidated. We showed recently that DHA, a 22-carbon chain omega-3 fatty acid found abundantly in oily fish such as herring, salmon, and sardine (28), robustly and reversibly activates vascular Slo1+β1 channels and that this modulatory phenomenon underlies the hypotensive effect of DHA injection observed in mice (27). Biophysically, DHA destabilizes the closed conformation of the ion conduction gate of the Slo1+β1 channel without any requirement for voltage-sensor activation

or Ca^{2+} binding, leading to a shift in half-activation voltage ($\Delta V_{0.5}$) of about −60 mV and acceleration of the activation kinetics (27). The results presented here show that the large effects of DHA on $\Delta V_{0.5}$ and activation kinetics are dependent on the auxiliary subunit composition; the effects are robust in Slo1+β1 and Slo1+β4 but significantly smaller in Slo1+β2, Slo1+LRRC26 (γ1), and Slo1 without any auxiliary subunits.

One potential confounding factor in studies using Slo1 channels with β subunits is incomplete coassembly of the subunits. In our study, the current-enhancing effect of DHA is not particularly noticeable in Slo1 channels without any auxiliary subunits coexpressed (Fig. 1 *B* and *C*). Thus, incomplete assembly of Slo1 and mutant β subunits, allowing channels without any β to conduct currents, may give an appearance that currents through the Slo1+mutant β channels are less responsive to DHA. We guarded against this possibility by ensuring that ionic currents through Slo1+β channels are significantly different from those through Slo1 channels. For example, the kinetics of ionic currents through Slo1+β1 R11A is clearly slower than that of Slo1 alone and virtually identical to that of Slo1+wild-type β1, indicating adequate coassembly of Slo1 and β1 R11A; yet, the effect of DHA in Slo1+β1 R11A is greatly diminished. Another strong line of evidence against the incomplete assembly idea comes from the fact that we were able to greatly augment the response to DHA in Slo1+β2 by making β2-to-β1/β2-to-β4 double mutations in the N terminus and TM1. Taken together, incomplete assembly of Slo1 and β subunits does not account for the differential effects of DHA on the Slo1 channel complexes with β1, β2, β4, or LRRC26 (γ1).

Arg11 and Cys18 in the N terminus and TM1 of β1, respectively, are crucial in supporting the large effects of DHA observed in Slo1+β1. Similar robust effects of DHA are observed when a pair of oppositely charged amino acids, specifically Arg and Glu, Lys and Asp, and Lys and Glu, irrespective of their order, is present at the aforementioned positions. Whereas the exact spatial arrangement of the residues at positions 11 and 18 in β1 is yet to revealed, it is possible that the side chains of the engineered positively charged and negatively charged residues are proximate enough to form a hydrogen bond or an electrostatic interaction. A similar interaction may exist between Glu12 and Arg19 in wild-type β4. Such an interaction may impose an additional degree of conformational constraint within the N terminus and the cytoplasmic end of TM1. Whether a direct and close interaction between Arg11 and Cys18 of wild-type β1 exists remains to be elucidated. The side chain of free cysteine has a pK_a value of 8–9 (37) but it can be significantly lower in some protein environments, especially near the N termini of α-helices, so that the side chain may bear a partial negative charge (38, 39). The side chain of Cys18, located near the N-terminal end of TM1 in β1, could be ionized ($thionate^-$) and may interact directly with the positively charged side chain of Arg11. This interaction may underlie the large $\Delta V_{0.5}$ by DHA in Slo1+β1. One observation that is not readily reconciled with the electrostatic interaction postulate is the large $\Delta V_{0.5}$ by DHA in Slo1+β1 C18R with Arg at position 11. This may suggest that the side chains of the residues at positions 11 and 18 are not exclusive partners but capable of interacting with others; for instance, in β1 C18R, the side chain of Arg18 may interact with Glu13 or a nearby backbone carbonyl group.

How Arg11 in the N terminus and Cys18 in TM1 of β1 contribute to the augmented response to DHA in the Slo1+β1 complex is not clear. Systematic cross-linking studies suggest that TM1 faces S1 and S2 of a pore-forming Slo1 subunit and TM2 faces S0 of a neighboring Slo1 subunit at the extracellular side (16). If this spatial arrangement is maintained at the intracellular side, the intracellular side of TM1 may be within 20–30 Å of the inner pore helix S6 and the S6-RCK1 linker, both of which are known structural components contributing to gating of the channel (40–42). The N terminus of β1 probably contains ∼16 amino acid residues and its length could be up to 50 Å in the most extended conformation. Thus, a direct interaction between S6 and the TM1 N terminus may be possible to destabilize the closed state and increase open probability (27).

Whereas the responses of Slo1+β1 and Slo1+β4 channels to DHA are much greater, a small but noticeable increase in ionic current through Slo1 channels without any auxiliary subunits was observed (Fig. 1 *B* and *C*). This may suggest that the Slo1 protein itself harbors sensors for DHA and that the presence of β1 or β4 tremendously potentiates functional coupling of DHA binding to the ion conduction gate of the Slo1 channel. The arrangement in which the consequence of binding of a ligand to Slo1 itself is augmented by the presence of a specific β subunit is also seen with PIP_2, a lipid messenger. Exogenously applied PIP_2 most probably binds to the sequence RKK in the S6-RCK1 linker segment of Slo1 and increases open probability appreciably when β1 is coexpressed but the increase is noticeably smaller with β4 (24). The relative ineffectiveness of PIP_2 with Slo1+β4 channels, however, is in contrast with the finding described here that β1 and β4 are equally effective in supporting the large effects of DHA.

The augmentation of the response to DHA binding observed in vascular Slo1+β1 channels involving Arg11 and Cys18 in the N terminus and TM1 of β1 respectively underlies the robust hypotensive effect of DHA observed in mice (27). Our observation that DHA also markedly activates Slo1+β4 channels, which are expressed abundantly in the nervous system (2, 43), suggests that DHA-mediated modulation of neuronal BK channels plays yet to be discovered physiologically and pathophysiologically important roles in the nervous system.

Tissue-specific coassembly of Slo1 and its auxiliary subunits contributes to the remarkable diversity of BK channels (2, 4). Our finding that DHA preferentially activates Slo1+β1 and Slo1+β4 channels among Slo1 complexes with different subunit compositions suggests that Slo1 BK channels are effectors of DHA with high tissue specificity.

Materials and Methods

Channel Expression. Human large-conductance Ca^{2+}- and voltage-dependent Slo1 K^+ channels (KCNMA1, AAB65837) and their auxiliary subunits β1 (KCNMB1, NP_004128), β2 (KCNMB2, NP_852006), β4 (KCNMB4, AAF69805), and LRRC26 (NP_001013675) were expressed in HEK cells by DNA transfection using FuGene 6 (Promega) (44). In most of the experiments described, β subunits with EGFP fused to the C terminus (pcDNA3.1/CT-GFP-TOPO; Life Technologies) with a 17-residue-long linker were used. Similar results were obtained with β1 and β1-EGFP and with β4 and β4-EGFP. Some of the chimeric constructs were based on those already described (45, 46). For those experiments involving coexpression of Slo1 and an auxiliary subunit, the DNA weight ratio in transfection was typically 1:1. Functional coassembly with the auxiliary subunits was confirmed in each patch by the characteristically altered gating properties conferred (3, 21, 44–46). Electrophysiological characteristics of ionic currents recorded from cells transfected with Slo1 and various auxiliary subunit DNAs together were clearly different from those of Slo1 currents without any auxiliary subunits (Figs. S1–S3), suggesting adequate coassembly of Slo1 and the auxiliary subunits.

Electrophysiology and Analysis. Currents were recorded using the inside-out patch-clamp method with an AxoPatch 200A or 200B amplifier (Molecular Devices) at room temperature. Dental wax or Sylgard-coated borosilicate electrodes had a typical initial resistance of 0.6–2 MΩ, and ∼60% of the resistance was electronically compensated. An effort was made to form GΩ seals as rapidly as possible without much negative pressure. The channels in membrane patches obtained in such a manner responded to DHA rapidly and reversibly. The output of the patch-clamp amplifier was filtered through the built-in 10-kHz filter of the amplifier, digitized, and analyzed as described using custom routines running in Igor Pro (WaveMetrics) (47). The external solution contained (in millimolars): 140 KCl, 2 $MgCl_2$, 10 Hepes, pH 7.2 with *N*-methyl-D-glucamine (NMG). The internal solution without Ca^{2+} contained (in millimolars): 140 KCl, 11 EGTA, 0.02 18C6TA, and 10 Hepes with NMG. Internal solutions with greater concentrations of free Ca^{2+} were prepared using various amounts of EGTA or HEDTA and added $CaCl_2$ as appropriate (47). The solutions with $[Ca^{2+}] \geq 100$ μM did not contain any chelator. For each channel type, voltage pulse durations were adjusted to

allow for steady-state measurements. Unless otherwise noted, the holding voltage was 0 or –30 mV. Normalized conductance-voltage curves were constructed from extrapolated instantaneous tail current amplitudes (I_{max} (0, V_m)), and the voltage dependence in each data set was in turn fitted with the following data description equation:

$$\frac{G(V_m)}{G_{max}} = \left(\frac{I(0,V_m)}{I_{max}(0)}\right)\left(\frac{1}{1+e^{-(V_m-V_{0.5})\left(\frac{Q_{app}F}{RT}\right)}}\right),$$

where $G(V_m)/G_{max}$ represents the normalized conductance at the membrane potential V_m. F, R, and T have their usual meanings. The values of maximal instantaneous tail current size ($I_{max}(0)$), half-activation voltage ($V_{0.5}$), and the number of equivalent charges (Q_{app}) were estimated from $I(0, V_m)$. In each patch, changes in voltage dependence of activation by DHA were described by changes in half-activation voltage ($\Delta V_{0.5}$) and the fractional change in apparent charge movement (Q_{app} ratio). Estimated equation parameters are presented as mean ± 95% confidence interval as implemented in IgorPro. Time courses of Slo1 currents were characterized by single exponentials. Time constant values were estimated from fitting the currents elicited by pulses to the voltages indicated (triangles in all figures) or the currents measured at the voltages indicated following pulses to a depolarized voltage, typically >200 mV (inverse triangles in all figures). In some patches, the effect of DHA diminished with time and these results were not included in our analysis.

Reagents. DHA was obtained from Sigma and Avanti. The stock solution in ethanol was stored in glass vials at –20 °C and diluted to the final concentrations immediately before experiments by vigorous vortexing. DHA was applied at 3 μM and ethanol at the concentration used (<0.01%) had no effect.

Statistics. The numbers of independent measurements are indicated in the figures. Statistical results in the text are presented as mean ± SEM (n), where n is the number of independent measurements. The Mann–Whitney or Wilcoxon test with an α level of 0.05, which was corrected for multiple comparisons using the Bonferroni method when appropriate, was used to evaluate statistical significance.

ACKNOWLEDGMENTS. We thank Profs. Latorre and Lingle for some of the chimeric constructs used in the study. This work was supported by the public in part through the National Institutes of Health (R01GM057654), German Research Foundation (FOR 1738), National Natural Science Foundation of China (31271217), and Key Project of Shanghai Science and Technology Commission (11JC1406400).

1. Salkoff L, Butler A, Ferreira G, Santi C, Wei A (2006) High-conductance potassium channels of the SLO family. *Nat Rev Neurosci* 7(12):921–931.
2. Wu RS, Marx SO (2010) The BK potassium channel in the vascular smooth muscle and kidney: α- and β-subunits. *Kidney Int* 78(10):963–974.
3. Yan J, Aldrich RW (2010) LRRC26 auxiliary protein allows BK channel activation at resting voltage without calcium. *Nature* 466(7305):513–516.
4. Yan J, Aldrich RW (2012) BK potassium channel modulation by leucine-rich repeat-containing proteins. *Proc Natl Acad Sci USA* 109(20):7917–7922.
5. Brenner R, Jegla TJ, Wickenden A, Liu Y, Aldrich RW (2000) Cloning and functional characterization of novel large conductance calcium-activated potassium channel β subunits, hKCNMB3 and hKCNMB4. *J Biol Chem* 275(9):6453–6461.
6. Behrens R, et al. (2000) hKCNMB3 and hKCNMB4, cloning and characterization of two members of the large-conductance calcium-activated potassium channel β subunit family. *FEBS Lett* 474(1):99–106.
7. Knaus HG, Garcia-Calvo M, Kaczorowski GJ, Garcia ML (1994) Subunit composition of the high conductance calcium-activated potassium channel from smooth muscle, a representative of the mSlo and slowpoke family of potassium channels. *J Biol Chem* 269(6):3921–3924.
8. Nelson MT, Bonev AD (2004) The β1 subunit of the Ca^{2+}-sensitive K^+ channel protects against hypertension. *J Clin Invest* 113(7):955–957.
9. Brenner R, et al. (2000) Vasoregulation by the β1 subunit of the calcium-activated potassium channel. *Nature* 407(6806):870–876.
10. Petkov GV, et al. (2001) β1-subunit of the Ca^{2+}-activated K^+ channel regulates contractile activity of mouse urinary bladder smooth muscle. *J Physiol* 537(Pt 2):443–452.
11. Meredith AL, Thorneloe KS, Werner ME, Nelson MT, Aldrich RW (2004) Overactive bladder and incontinence in the absence of the BK large conductance Ca^{2+}-activated K^+ channel. *J Biol Chem* 279(35):36746–36752.
12. Seibold MA, et al. (2008) An African-specific functional polymorphism in KCNMB1 shows sex-specific association with asthma severity. *Hum Mol Genet* 17(17):2681–2690.
13. Knaus HG, Eberhart A, Kaczorowski GJ, Garcia ML (1994) Covalent attachment of charybdotoxin to the β-subunit of the high conductance Ca^{2+}-activated K^+ channel. Identification of the site of incorporation and implications for channel topology. *J Biol Chem* 269(37):23336–23341.
14. Wang YW, Ding JP, Xia XM, Lingle CJ (2002) Consequences of the stoichiometry of Slo1 α and auxiliary β subunits on functional properties of large-conductance Ca^{2+}-activated K^+ channels. *J Neurosci* 22(5):1550–1561.
15. Wu RS, et al. (2009) Location of the β4 transmembrane helices in the BK potassium channel. *J Neurosci* 29(26):8321–8328.
16. Liu G, et al. (2010) Location of modulatory β subunits in BK potassium channels. *J Gen Physiol* 135(5):449–459.
17. Morera FJ, et al. (2012) The first transmembrane domain (TM1) of β2-subunit binds to the transmembrane domain S1 of α-subunit in BK potassium channels. *FEBS Lett* 586(16):2287–2293.
18. Wallner M, Meera P, Toro L (1999) Molecular basis of fast inactivation in voltage and Ca^{2+}-activated K^+ channels: A transmembrane β-subunit homolog. *Proc Natl Acad Sci USA* 96(7):4137–4142.
19. Uebele VN, et al. (2000) Cloning and functional expression of two families of β-subunits of the large conductance calcium-activated K^+ channel. *J Biol Chem* 275(30): 23211–23218.
20. Orio P, Latorre R (2005) Differential effects of β1 and β2 subunits on BK channel activity. *J Gen Physiol* 125(4):395–411.
21. Bao L, Cox DH (2005) Gating and ionic currents reveal how the BK_{Ca} channel's Ca^{2+} sensitivity is enhanced by its β1 subunit. *J Gen Physiol* 126(4):393–412.
22. McManus OB, et al. (1995) Functional role of the β subunit of high conductance calcium-activated potassium channels. *Neuron* 14(3):645–650.
23. Valverde MA, et al. (1999) Acute activation of Maxi-K channels (hSlo) by estradiol binding to the β subunit. *Science* 285(5435):1929–1931.
24. Vaithianathan T, et al. (2008) Direct regulation of BK channels by phosphatidylinositol 4,5-bisphosphate as a novel signaling pathway. *J Gen Physiol* 132(1):13–28.
25. McManus OB, et al. (1993) An activator of calcium-dependent potassium channels isolated from a medicinal herb. *Biochemistry* 32(24):6128–6133.
26. King JT, et al. (2006) β2 and β4 subunits of BK channels confer differential sensitivity to acute modulation by steroid hormones. *J Neurophysiol* 95(5):2878–2888.
27. Hoshi T, et al. (2013) Omega-3 fatty acids lower blood pressure by directly activating large-conductance Ca^{2+}-dependent K^+ channels. *Proc Natl Acad Sci USA* 110:4816–4821.
28. Mozaffarian D, Wu JH (2011) Omega-3 fatty acids and cardiovascular disease: Effects on risk factors, molecular pathways, and clinical events. *J Am Coll Cardiol* 58(20):2047–2067.
29. Saravanan P, Davidson NC, Schmidt EB, Calder PC (2010) Cardiovascular effects of marine omega-3 fatty acids. *Lancet* 376(9740):540–550.
30. Bradbury J (2011) Docosahexaenoic acid (DHA): An ancient nutrient for the modern human brain. *Nutrients* 3(5):529–554.
31. Lafourcade M, et al. (2011) Nutritional omega-3 deficiency abolishes endocannabinoid-mediated neuronal functions. *Nat Neurosci* 14(3):345–350.
32. Gören JL, Tewksbury AT (2011) The use of omega-3 fatty acids in mental illness. *J Pharm Pract* 24(5):452–471.
33. Swanson D, Block R, Mousa SA (2012) Omega-3 fatty acids EPA and DHA: Health benefits throughout life. *Adv Nutr* 3(1):1–7.
34. Torres YP, Morera FJ, Carvacho I, Latorre R (2007) A marriage of convenience: β-subunits and voltage-dependent K^+ channels. *J Biol Chem* 282(34):24485–24489.
35. Xia XM, Ding JP, Lingle CJ (2003) Inactivation of BK channels by the NH_2 terminus of the β2 auxiliary subunit: An essential role of a terminal peptide segment of three hydrophobic residues. *J Gen Physiol* 121(2):125–148.
36. Knaus HG, et al. (1994) Primary sequence and immunological characterization of β-subunit of high conductance Ca^{2+}-activated K^+ channel from smooth muscle. *J Biol Chem* 269(25):17274–17278.
37. Lindley H (1960) A study of the kinetics of the reaction between thiol compounds and choloracetamide. *Biochem J* 74:577–584.
38. Kortemme T, Creighton TE (1995) Ionisation of cysteine residues at the termini of model α-helical peptides. Relevance to unusual thiol pK_a values in proteins of the thioredoxin family. *J Mol Biol* 253(5):799–812.
39. Madzelan P, Labunska T, Wilson MA (2012) Influence of peptide dipoles and hydrogen bonds on reactive cysteine pK_a values in fission yeast DJ-1. *FEBS J* 279(22):4111–4120.
40. Niu X, Qian X, Magleby KL (2004) Linker-gating ring complex as passive spring and Ca^{2+}-dependent machine for a voltage- and Ca^{2+}-activated potassium channel. *Neuron* 42(5):745–756.
41. Wu Y, et al. (2009) Intersubunit coupling in the pore of BK channels. *J Biol Chem* 284(35):23353–23363.
42. Chen X, Aldrich RW (2011) Charge substitution for a deep-pore residue reveals structural dynamics during BK channel gating. *J Gen Physiol* 138(2):137–154.
43. Brenner R, et al. (2005) BK channel β4 subunit reduces dentate gyrus excitability and protects against temporal lobe seizures. *Nat Neurosci* 8(12):1752–1759.
44. Hou S, et al. (2011) Bilirubin oxidation end products directly alter K^+ channels important in the regulation of vascular tone. *J Cereb Blood Flow Metab* 31(1):102–112.
45. Orio P, et al. (2006) Structural determinants for functional coupling between the β and α subunits in the Ca^{2+}-activated K^+ (BK) channel. *J Gen Physiol* 127(2):191–204.
46. Zeng XH, Xia XM, Lingle CJ (2003) Redox-sensitive extracellular gates formed by auxiliary β subunits of calcium-activated potassium channels. *Nat Struct Biol* 10(6): 448–454.
47. Hou S, Xu R, Heinemann SH, Hoshi T (2008) Reciprocal regulation of the Ca^{2+} and H^+ sensitivity in the SLO1 BK channel conferred by the RCK1 domain. *Nat Struct Mol Biol* 15(4):403–410.